Antiproton radiation belt produced by cosmic rays in the Earth's magnetosphere

Anatoly A. Gusev,[1] Udaya B. Jayanthi, and Kenny T. Choque
National Institute for Space Research, INPE, Sao Jose dos Campos, Brazil

Galina I. Pugacheva and Nelson Schuch
Southern Regional Space Research Center/INPE, Santa Maria, Brazil

Walther N. Spjeldvik
Department of Physics, Weber State University, Ogden, Utah, USA

Received 21 August 2002; revised 1 December 2002; accepted 20 January 2003; published 20 February 2003.

[1] The possible existence of noticeable fluxes of antiparticles in the Earth magnetosphere has been predicted on theoretical considerations in this article. The antiprotons expected at several hundred kilometers of altitudes, we do not believe are of direct extraterrestrial origin, but are the natural products of nuclear reactions of the high-energy primary cosmic rays (CR) with the constituents of the terrestrial atmosphere. Extraterrestrial, galactic antiprotons are themselves of secondary in origin, i.e. they are born in nuclear reactions of the same CR particles passing through 5–7 g/cm^2 of interstellar matter encountered during their lifetime in the Galaxy. We expect that the fluxes of magnetospheric antiprotons to be higher compared to the interstellar fluxes because the fluxes get accumulated due to confinement by the magnetic field of the Earth. We present the results of the computations of the antiproton fluxes at 50 MeV to several GeV energies due to the CR particle interactions with the matter in the interstellar space, and also with the residual atmosphere at altitudes of ~1000 km over the Earth's surface. The estimates show that the magnetospheric antiproton fluxes are two orders of magnitude greater compared to the interstellar fluxes measured at energies < 1 GeV. INDEX TERMS: 2104 Interplanetary Physics: Cosmic rays; 2720 Magnetospheric Physics: Energetic particles, trapped; 7859 Space Plasma Physics: Transport processes; 2753 Magnetospheric Physics: Numerical modeling; 0355 Atmospheric Composition and Structure: Thermosphere—composition and chemistry. **Citation:** Gusev, A. A., U. B. Jayanthi, and K. T. Choque, Antiproton radiation belt produced by cosmic rays in the Earth magnetosphere, *Geophys. Res. Lett.*, *30*(4), 1161, doi:10.1029/2002GL016146, 2003.

1. Introduction

[2] Measurements of the interstellar antiproton spectrum generally support the idea of their secondary origin i.e. they are produced in nuclear reactions with the interstellar matter by the primary cosmic rays (CR) in their chaotic motion in the galactic magnetic field during their lifetime in Galaxy. The same nuclear reactions of cosmic ray protons that occur in the interstellar media also happen in the Earth's atmosphere, including the uppermost residual atmosphere corresponding to high altitudes. In these nuclear reactions a great variety of secondary particles are produced, including antiprotons. Part of these particles born in the confinement region of the magnetosphere will be trapped in the Earth's vicinity by geomagnetic field creating an antiproton radiation belt around the Earth. This belt is a product of the nuclear reactions similar to those of positron and isotope radiation belts [*Gusev et al.*, 2001; *Pugacheva et al.*, 1998] created at the altitudes of about ~1000 km above the Earth. The estimates of the trapped antiproton fluxes at these altitudes in the equatorial region, where the atmospheric density is very small (~$5\cdot10^{-18}$–10^{-17} g/cm^3) but in comparison much greater than the ~$1.7\cdot10^{-24}$ g/cm^3 of interstellar matter, are obtained.

2. Antiproton Production Spectrum

[3] The minimum kinetic proton energy for the production of an antiproton in the reaction $p + p \rightarrow p + p + p + \tilde{p}$, a kinematic threshold is $E_{th} = 6m_p = 5629$ MeV in the case of the hydrogen target and $E_{th} = (2 + 4/A)m_p$ in the $p + A$ reaction [*Gaisser and Levy*, 1974], where A is a target nucleus atomic mass. We consider here essentially the antiproton production by the cosmic ray protons. The CR helium nuclei also contribute to the antiproton production by about ~25%.

[4] For the modeling of the secondary nuclear reaction products, their spectra and angular distributions, the nuclear reaction computer code SHIELD [*Dementyev and Sobolevsky*, 1999] was used. The kinetic energy of the projectile in the range from several MeV to hundreds of GeV, can serve as an input to the code for targets with atomic mass $A \geq 1$. The simulations were performed to obtain spectra of the secondary antiprotons and antineutrons (which are also born in the analogues reaction $p + p \rightarrow p + p + n + \tilde{n}$) with energies of 1 MeV to 1000 GeV in reactions of projectile protons with energies of 6–1000 GeV against target nuclei of hydrogen, helium and oxygen. The results of the simulation are shown in Figures 1 and 2. Figure 1 shows the multiplicity (i.e. the number of certain type of particles born in a nuclear interaction) of antiprotons produced in (p, p), (p, He) and (p, O) nuclear reactions and its dependence on the projectile proton energy. The multiplicity sharply increases by several orders at energies above E_{th} for protons

[1] Also at Space Research Institute of Russian Academy of Sciences, Moscow, Russia.

0094-8276/03/2002GL016146

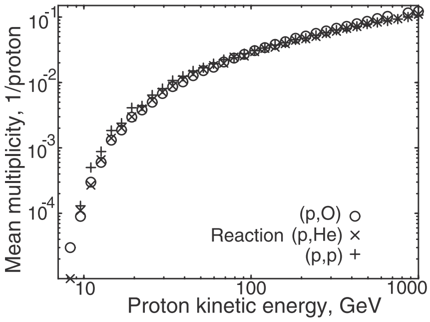

Figure 1. The antiproton multiplicity.

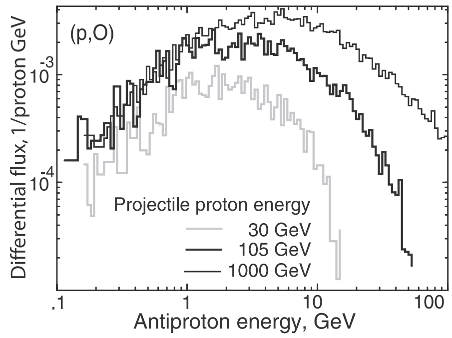

Figure 2. The differential antiproton production spectra generated by protons with energy E_p on O target atomic nucleus.

of ≈10 GeV incident on hydrogen target, and for protons of 8 to 9 GeV in case of *He* and *O* nucleus target, in agreement with the expression $E_{th} = (2 + 4/A)m_p$. The multiplicity is practically independent of the target atomic number and is greater for the antineutrons. The antiproton angle distribution is very narrow of ~5° around the incident proton velocity vector, in the laboratory system, for different energies of protons against *H*, *He* and *O* targets. The inelastic cross-section values $\sigma_{inel,}$ obtained with SHIELD code are in good agreement with the formula of *Letaw et al.*, [1983] for the (p, He) and (p, O) reactions and with that of *Tan and Ng*, [1982] for the (p, p) reaction.

[5] Figure give examples of the differential secondary antiproton production spectra $q(E_{\tilde{p}}, E_p)$, generated in 4π solid angle by one proton with energy E_p on one *H*, *He* or *O* target nucleus. The energy distributions from protons with $E_p \approx 30$ GeV exhibit the characteristic flat maximum between antiproton energies of 1–2 GeV as observed in the various experiments ([*Boezio et al.*, 2001] and references therein). This agreement indicates the secondary nature of the antiprotons observed and confirms the secondary antiproton spectrum calculations performed with SHIELD code. The heavier the target nucleus, the more abundant are the antiprotons at energies below 200 MeV. The elemental composition of interstellar matter for *H*, *He* and *O* is in the proportion 1:0.1:10^{-3} [*Simon, et al.*, 1998] compared to the 1.43:29.8:68.76 of the atmosphere at $L = 1.2$ (the MSIS86 atmospheric model densities averaged over confinement region with the characteristic parameter L). The antiprotons at energies below 200 MeV, are much less in the spectrum of the interstellar antiprotons as the main target atoms are of *H* in comparison with atmospheric origin antiprotons which have more abundant *O* atoms as a target. The antiproton production spectrum $Q_{\tilde{p}}(E_{\tilde{p}})$ from the CR proton spectrum dN/dE_p is obtained by numerical integration of the antiproton production spectrum $q(E\tilde{p}, E_p)$ over the CR spectra:

$$Q_{\tilde{p}}(E_{\tilde{p}}) = \xi \int_{E}^{\infty} q(E_{\tilde{p}}, E_p) \frac{dN}{dE_p} dE_p \qquad (1)$$

Here ξ is a heavy nuclei correction factor of 1.25 describing the antiproton input, which includes the CR helium contribution [*Sina et al.*, 2001].

[6] The CR proton spectrum from the balloon experiment CAPRICE [*Boezio et al.*, 1999] was utilized:

$$\frac{dN}{dE_p} = (1.1 \pm 0.11) \cdot 10^{-4} E_p^{-2.73 \pm 0.06} \quad 1/m^2 srsGeV \ for \ E_p > 20 GeV. \qquad (2)$$

The authors demodulated the measured spectrum for the solar activity and obtained the interstellar spectrum:

$$\frac{dN}{dR} = (2.72 \pm 0.02) \cdot 10^4 R^{-2.928 \pm 0.004} \quad 1/m^2 srsGeV \ for \ R = 1.7 - 200 GV. \qquad (3)$$

[7] A solar modulation effect on CR proton flux is appreciable, about 8.7% even at rigidity of ~50 GV, corresponding to the mean kinetic energy of CR proton spectrum above 20 GeV (E_p = 47.39 GeV).

3. Interstellar Antiproton Flux

[8] In the computations of the antiproton production spectra through equation 1 we utilized the interstellar proton spectrum (equation 3) and the CR proton spectrum modulated by solar activity (equation 2) to obtain the interstellar and the atmospheric antiproton production spectra respectively. Multiplying the integral (1) by factor $\sigma_{inel} N_A / A$ that takes into account the elemental composition of interstellar space and of the atmosphere (N_A is the Avogadro constant), the interstellar and the atmospheric antiproton production spectra per g/cm^2 of the matter are obtained separately (Figure 3). For the interstellar production spectrum, the secondary antineutrons were considered, as during their long lifetime of $\sim 10^7$ years in the Galaxy, they decay quickly ($\tau_{lifetime} = 887 \pm 2$ s) and produce antiprotons. However, the magnetospheric antineutrons leave the confinement region sooner and decay outside: even a 10 MeV antineutron travels a distance of $7R_E$ in the first splits of a second after production. The magnetospheric antiproton

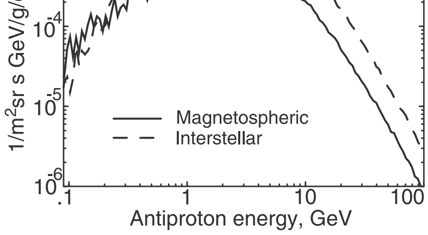

Figure 3. The computed antiproton production spectra.

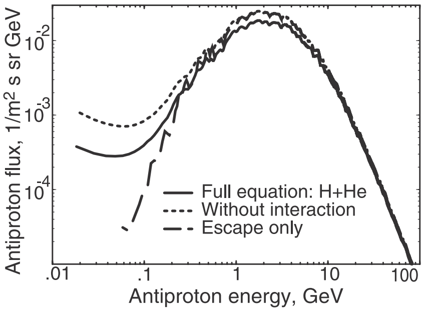

Figure 4. The computed interstellar antiproton flux.

production spectrum is more abundant with the lower energy antiprotons as we noted above due to the *O* target atoms (Figure 3).

[9] The interstellar antiproton flux is defined by a continuity equation related to the leaky-box model:

$$F_{\bar{p}}(E_{\bar{p}})/\lambda_{\rm esc} + F_{\bar{p}}(E_{\bar{p}})/\lambda_{\rm inel} + \frac{d}{dE_{\bar{p}}}\left(F_{\bar{p}}(E_{\bar{p}})\frac{dE_{\bar{p}}}{dX}\right) = Q_{\bar{p}}(E_{\bar{p}}) \qquad (4)$$

Here $\lambda_{\rm esc}$ is the escape length for leaky box model, from *Jones et al.*, [2001] and $\lambda_{\rm inel} = \sigma_{\rm inel}N_A/A$ is the interaction length of antiprotons in the Galaxy. The third term defines the antiproton ionization energy losses and $Q_{\bar{p}}(E_{\bar{p}})$ is an above mentioned antiproton production spectrum. The leaky box model considers a balance between the number of the particles born and lost due to escape from the Galaxy and to inelastic interactions with the interstellar matter, etc. and does not consider the diffusion process. The equation 4 was numerically solved with Runge-Kutta method and the computed interstellar antiproton flux is shown in Figures 4 and 5. The importance of the various interstellar processes and the parameters is demonstrated in Figure 4: for example, an antiproton nuclear interactions is not accounted (the dashed curve); the interactions and ionization losses are not accounted (the long dashed curve). In Figure 5 the computed interstellar antiproton flux is presented together with the results of recent balloon experiments. The experimental and modeling results are in satisfactory agreement, however we did not take into account a solar modulation of antiproton flux and the production of third generation of antiprotons due to inelastic scattering of the antiproton flux during its confinement time in the Galaxy.

4. The Earth's Antiproton Radiation Belt

[10] Encouraged by the good agreement between the simulated and the measured galactic antiproton fluxes, we adopted the same approach for modeling the magnetospheric trapped antiproton flux around L = 1.2 (i.e. at a typical altitude of $0.2R_{\rm E}$ above the Earth surface) in the geomagnetic equatorial region where the fluxes of other energetic species like positrons, light element isotope ions [*Pugacheva et al.*, 1998] and the 500 MeV trapped proton fluxes [AP-8 model, *Vette*, 1991] are also found to be maximum. The trapped particles at L = 1.2 possess a narrow pitch-angle distribution around 90° ± 20°. Thus, approximately all CR nuclei incident to L = 1.2 within the same angles produce antiprotons which will be trapped.

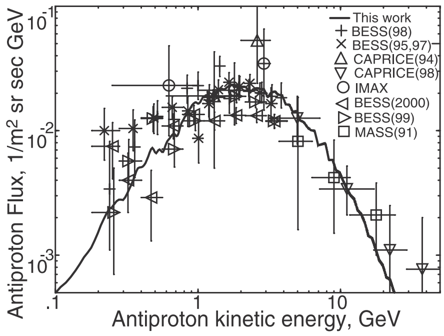

Figure 5. The comparison of the computed and measured galactic antiproton flux.

[11] The particles are considered as trapped forever in an ideal magnetic dipole when the gyration radius R_L around a given magnetic field line is less than $R_{\rm c}/10$, where $R_{\rm c}$ is the radius of curvature of the magnetic field line ($R_{\rm c} = R_{\rm E}L/3$ at the equatorial region). The antiprotons participate in the adiabatic motion in the magnetosphere, drifting on the same L-shell 1.2 around the Earth, and get accumulated in the magnetic cavity until the ionization losses and nuclear interactions remove them. They could be captured forever in the absence of those losses. From the criteria $R_{\rm c}/R_L \geq 10$, we estimate that antiprotons that could be trapped at L = 1.2 have maximum kinetic energy of $E_{\rm crit}$ = 1.0 GeV. The particles with greater energy have limited lifetime in the confinement region due to chaotic pitch-angle scattering process described by *Chirikov* [1978]. The corresponding escape length is defined as $\lambda_{\rm esc} = \upsilon\rho\tau_{\rm esc}$ where υ is an antiproton velocity and ρ is an atmospheric density at L = 1.2. A particle lifetime $\tau_{\rm esc}$ at given L-shell due to this process was estimated by *Pugacheva et al.*, [1996]. The $\lambda_{\rm esc}$ is equal to infinity for particle with energy below $E_{\rm crit}$ and equals to zero for the energies much greater than $E_{\rm crit}$. The atmospheric interaction length $\lambda_{\rm intr}$ and the antiproton ionization losses in atmosphere will be different from the interstellar case as the elemental composition of the media is different. The antineutron stopping power values for the different matters were obtained from American Institute of Standards http://physics.nist.gov/PhysRefData].

[12] In the modeling of the trapped magnetospheric antiproton flux we employed the same equation 4 with the parameters corresponding to the atmospheric elemental composition. The antiproton production spectrum shown in Figure 3 was utilized and the results of the numerical integration of equation 4 are shown in Figure 6. The

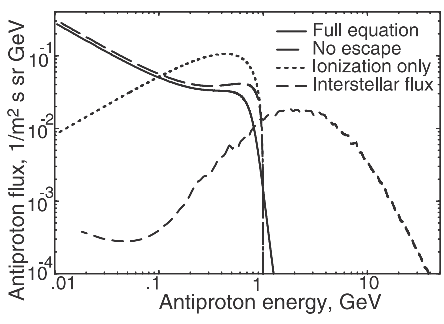

Figure 6. The magnetospheric antiproton flux at L = 1.2.

computed antiproton flux geomagnetically trapped in the radiation belt is compared with the interstellar fluxes in the same figure. The magnetospheric antiproton fluxes exhibit a soft spectrum, which sharply falls to zero at $\approx E_{\rm crit}$. At energies lower than 1–2 GeV the magnetospherically trapped antiproton fluxes are about 50–100 times greater than the interstellar fluxes.

[13] An importance of the various parameters is shown in Figure 6: if one neglects the antiproton interactions with the matter he gets several times overestimated antiproton trapped fluxes in the energy range of 0.1–1 GeV (the dotted line); if we do not introduce $\lambda_{\rm esc}$ and choose a cut-off in the antiproton production spectrum at energies greater than $E_{\rm crit}$ (considering that they can not be trapped), the result will be almost the same (the long dashed line) as for full equation 4 solution (the solid line).

[14] The spread of the antiproton belt flux modeled here at L = 1.2 is very narrow, it will decrease sharply with increasing L due to less atmospheric matter: the lower the atmospheric density the greater is the time necessary to create and accumulate flux. Theoretically the lifetime approximates slowly to the antiproton lifetime in the Galaxy, however in reality the geomagnetic disturbances in the Earth's inner magnetosphere limit the lifetime of particles to several years.

[15] The atmospheric layer of about 90 g/cm^2 of thickness is a source of albedo neutrons and antineutrons. These antineutrons decay into antiprotons and can contribute to the antiproton radiation belt fluxes modeled above. In this first approach of antiproton belt modeling we neglect the contribution from the albedo antineutrons, and we will consider it later.

5. Conclusion

[16] The modeling considered here for the production of antiprotons utilized nuclear interactions between cosmic ray nuclei with energies above the reaction threshold of 6 GeV and the constituents of the environment. Initially, we proceeded with the production of antiprotons in interstellar space and conferred with the balloon measurements. In the next step, we calculated the antiproton contribution due to the cosmic ray nuclei interactions with the atmospheric constituents H, He and O species at altitudes of L = 1.2 in the near Earth environment, to examine the viability of the formation of an antiproton belt. We obtained large fluxes compared to the interstellar fluxes by factors 50 to 100 at energies <1 GeV. However, during strong geomagnetic storms the trapped radiation can be scattered into lower atmospheric altitudes of the same L-shells or dislocate to other L-shells which could possibly contaminate interstellar flux measurements.

[17] The model estimates of the antiproton fluxes obtained here for the inner magnetosphere can be verified in the near future by the planned AMS experiment which is scheduled for installation on the International Space Station for antiparticle - antimatter measurements [*The AMS Collaboration*, 2000]. These experiments that can be envisaged on board LEO satellite missions can monitor the interstellar antiproton flux at high latitudes and the magnetospheric antiproton fluxes at the low latitudes in their orbits. This modeling of an antiproton radiation belt is useful for space engineering and scientific applications.

[18] **Acknowledgments.** Dr. A.A. Gusev and Mr. K. Choque thank the CNPq for the fellowships and Dr. G. I. Pugacheva acknowledges the support from FAPERGS.

References

Boezio, M., et al., The cosmic ray proton spectra between 0.4 and 200 GV, *Astrophys. J*, *518*, 457–472, 1999.

Boezio, M., et al., High-energy cosmic-ray antiprotons with the CAPRICE98 experiment, paper presented at 27th International Cosmic Ray Conference, Hamburg, Germany, 7–15 Aug. 2001.

Chirikov, B. V., The stability problem of charge particle motion in magnetic trap, *Sov. J. Plasma Phys.*, *4*, 289, 1978.

Dementyev, A. V., and N. M. Sobolevsky, SHIELD-Universal Monte Carlo Hadron Transport Code: Scope and applications, *Radiat. Meas.*, *30*, 553, 1999.

Gaisser, T. K., and E. N. Levy, Astrophysical implications of cosmic ray antiprotons, *Phys. Rev. D*, *10*, 1731–1735, 1974.

Gusev, A. A., U. B. Jayanthi, I. M. Martin, G. I. Pugacheva, and W. N. Spjeldvik, Nuclear reactions on rarest atmosphere as a source of magnetospheric positron radiation belt, *J. Geophys. Res.*, *106*(A11), 26,111–26,116, 2001.

Jones, F. C., A. Lukasiak, and V. S. Ptuskin, The modified weighted Slab technique: Models and results, *Astrophys. J.*, *547*, 264–271, 2001.

Letaw, J. R., R. Silberberg, and C. H. Tsao, Proton nucleus total inelastic cross sections: An empirical formula for E > 10 MeV, *Astrophys. J. Suppl. Ser.*, *51*, 271–275, 1983.

Pugacheva, G. I., et al., On the chaos and stability problem in the trapping of anomalous cosmic ray heavy ions by the Earth's magnetosphere, *Planet. Space Sci.*, *44*, 267–271, 1996.

Simon, M., A. Molharan, and S. Roesler, A new calculations of the interstellar secondary cosmic ray antiprotons, *Astrophys. J.*, *499*, 250–257, 1998.

Sina, R., V. S. Ptuskin, and E. S. Seo, Antiproton spectrum in the galactic wind model, *Adv. Space Res.*, *27*(4), 705–710, 2001.

Pugacheva, G. I., et al., Hydrogen and helium isotope inner radiation belts in the Earth's magnetosphere, *Ann. Geophys.*, *16*, 931–939, 1998.

Tan, L. C., and L. K. Ng, Parametrization of pbar invariant cross-section in p-p collisions using a new scaling variable, *Phys. Rev. D*, *26*, 1179–1182, 1982.

The AMS Collaboration, Protons in near Earth orbit, *Phys. Lett. B*, *472*, 215–226, 2000.

Vette, J. I., The NASA/National Space Science Data Center Trapped Radiation Environment Model Program (TREMP), *Rep. NSSDC/WDC 91–29*, NASA Goddard Space Flight Cent., Greenbelt, Md., 1991.

A. A. Gusev, U. B. Jayanthi, and K. T. Choque, National Institute for Space Research, INPE, Sao Jose dos Campos, Brazil.

G. I. Pugacheva and N. Schuch, Southern Regional Space Research Center/INPE, Santa Maria, Brazil.

W. N. Spjeldvik, Department of Physics, Weber State University, Ogden, Utah, USA.